Green Chemistry

PAPER

View Article Online
View Journal

Cite this: DOI: 10.1039/d0gc00793e

Non-ionic hydrophobic eutectics – versatile solvents for tailored metal separation and valorisation†

Nicolas Schaeffer, *[a] João H. F. Conceição,[a] Mónia A. R. Martins,[a] Márcia C. Neves,[a] Germán Pérez-Sánchez,[a] José R. B. Gomes,[a] Nicolas Papaiconomou[b] and João A. P. Coutinho *[a]

In comparison with the well-described ionic eutectic mixtures, hydrophobic eutectic solvents (HESs) composed of two non-ionic compounds represent a relatively new class of eutectics. In this work, a number of non-ionic HESs liquid at room temperature were identified from a large initial screening of potential mixtures. Three new HESs based on thymol + TOPO (trioctylphosphine oxide), TOPO + capric acid and hydrocinnamic acid + capric acid were investigated as extracting media for the recovery and separation of platinum group and transition metals in HCl media. Full phase diagrams and physical properties including viscosities, densities, chemical stability and the influence of water were characterised, with these HESs presenting low viscosities and high hydrophobicity suitable for application as solvents for liquid–liquid extraction. By simple variation of the eutectic component the selectivity of the system for a given metal could be tuned, with the TOPO-based system displaying good to excellent selectivity towards Pt^{4+}, Pd^{2+} and Fe^{3+} under a range of conditions. The extraction mechanism was found to vary due to a complex interplay between the HES composition, acid concentration and the predominant metal complex present. The observed extraction behaviour in HESs composed of two metal complexing ligands such as TOPO + capric acid, in which each respective component is responsible for metal extraction under given conditions, opens the possibility to design hydrophobic eutectic mixtures presenting synergistic effects. Finally, the HES phase following palladium extraction was used as the template for the formation of palladium nanoparticles. The results presented highlight the great potential of HESs as environmentally benign and tuneable media for the solvent extraction of metal ions.

Received 4th March 2020,
Accepted 27th March 2020

DOI: 10.1039/d0gc00793e

rsc.li/greenchem

Introduction

First proposed by Abbott and co-workers, deep eutectic solvents (DESs) are low-melting liquid mixtures composed of weak Lewis or Brønsted acids and bases.[1] The simple preparation and versatile properties of DESs, which can be freely modulated by careful selection of the hydrogen bond donor (HBD) and acceptor (HBA) as well as their respective ratio, have resulted in their widespread application as a templating solvent for material synthesis,[2,3] as media for metal–organic synthesis,[4] catalysis,[5] metal and biomass processing and gas adsorption to name but a few examples.[6–8] Despite their great compositional diversity, most reported DESs can be classified into five main types based on their constituents,[6,9] namely,

(1) Type I – quaternary ammonium halide salt + metal chloride;

(2) Type II – quaternary ammonium halide salt + metal chloride hydrate;

(3) Type III – quaternary ammonium halide salt + hydrogen bond donor;

(4) Type IV – metal chloride hydrate + hydrogen bond donor;

(5) Type V – hydrogen bond donor + hydrogen bond acceptor.

The ionic nature of Type I to IV DESs has greatly expanded the field of metal processing in non-aqueous media under ambient conditions, allowing for leaching[10,11] and electrodeposition processes[6,12] not typically feasible in water whilst providing a cost-efficient alternative to ionic liquids (ILs). In fact, metal complexation observed in Type I to IV DESs is domi-

[a]CICECO, Aveiro Institute of Materials, Department of Chemistry, University of Aveiro, Campus Universitário de Santiago, 3810-193 Aveiro, Portugal. E-mail: nicolas.schaeffer@ua.pt, jcoutinho@ua.pt
[b]Université Nice Sophia Antipolis, Department of Chemistry, 28 Avenue Valrose, 06103 Nice, France

†Electronic supplementary information (ESI) available. See DOI: 10.1039/d0gc00793e

nated by metal–halide anion interactions (typically chloride), and to a lesser extent oxo-metal interactions in Type III DESs, to form anionic halometallate complexes akin to those observed in halide-based ILs.[13] More recently, the applicability of DESs to metal processing was extended to solvent extraction with the introduction of hydrophobic eutectic solvents (HESs).[14] Despite their potential, the field is still in its infancy as evidenced by the limited number of publications to date; representative works using HESs for the solvent extraction of metal ions are summarised in Table S1 of the ESI.† Unfortunately, few works describe the full HES solid–liquid phase diagram or address the selectivity of the proposed extraction system, focusing instead on the extraction efficiency for one metal ion in the presence of various impurities.[15–18]

Most HES extraction studies focus on Type III eutectics based on mixtures of bulky quaternary ammonium or phosphonium halide ILs as HBAs and hydrophobic carboxylic acids as HBDs. Despite their successful extraction of In^{3+}, TcO_4^- and CrO_4^{2-},[16,17,19,20] the advantage of using such ionic HESs over hydrophobic ILs is not immediately obvious as they suffer from the same drawbacks as the ILs of which they are composed, namely higher viscosities, cost and toxicity.[21] Ionic compounds are inherently more water soluble than their non-ionic equivalents such that an IL cation with large alkyl moieties is required to confer sufficient hydrophobicity to the HES, thereby significantly increasing the HES toxicity.[22] Electrostatic interactions dominate both physico-chemical properties and the metal extraction mechanism in ionic HESs, resulting in relatively viscous HES mixtures which extract anionic metal complexes *via* an ion-exchange mechanism. HESs composed of an easily ionizable amine constituent such as lidocaine ($C_{14}H_{22}N_2O$) can also be included in the category of ionic HESs as their protonation under acidic conditions increases their water solubility and negatively impacts their recyclability.[23]

Non-ionic HESs overcome the issues associated with their ionic counterparts by removing coulombic interactions. Examples include mixtures of two different bio-sourced terpenes[24] as well as mixtures where a non-ionic metal complexing ligand is introduced as a constituent of the HES such as mixtures of thymol or menthol with carboxylic acids[25,26] or trioctylphosphine oxide (TOPO) with phenol.[27] The formation of fully organic HESs presenting large deviations from ideality, recently classified as Type V DESs, results from a strong interaction stemming from the acidity difference of the hydrogen bond donor and the hydrogen bond accepting moiety as in the case of the thymol + menthol system.[9] Such HESs present interesting properties relevant for solvent extraction processes, including low to extremely low water solubilities and lower viscosities (typically below 50 mPa s at room temperature), allowing for faster mass transfer properties, and densities sufficiently different to that of water for efficient phase demixing (in the range 0.90 to 0.95 g cm^{-3}).[24–27] The TOPO + phenol system successfully extracted uranyl cations from nitric acid solutions[27] whilst the thymol + capric acid mixture displayed good selectivity towards Fe^{3+} and Cu^{2+} over other transition metals.[26] In both systems, metal extraction proceeded similarly to that of pure TOPO or capric acid in organic diluents, suggesting that non-ionic extractants can be incorporated in Type V HESs whilst retaining their extraction properties. This results in potentially significant environmental benefits by substituting organic diluents traditionally used in solvent extraction by HESs containing non-ionic extractants present in concentrations far above those that can be achieved in most organic solvents.[27]

Platinum-group metals (PGMs), which include platinum and palladium, are well-known catalysts enabling many industrial processes, most notably in the reduction of automotive combustion emission. The economic importance of PGMs, their limited geographic availability and low ore grades of just a few grams per tonnes resulted in PGMs being included in the list of critical raw materials defined by the European Commission.[28,29] This criticality is further compounded by the forecasted growth in PGM usage within the next 20 years by possibly as much as 45% for Pd and 5% for Pt.[30] The increasing demand for PGMs combined with the large environmental impact associated with primary PGM extraction, estimated at 380 000 tonnes of material inputs per tonne of PGMs,[31] reinforces the need for versatile and environmentally benign extraction processes suitable for the recovery of PGMs from primary and secondary sources such as three-way catalysts and electronic waste.[32]

In this work, the potential of non-ionic HESs as selective extraction solvents for the recovery and separation of PGMs and the transition metals (TMs) copper, iron, chromium, nickel, and cobalt in HCl media, is investigated. A large screening of potential new HES mixtures was performed according to a protocol similar to that established by van Osch and co-workers.[33] Based on the stability of these novel HESs under acidic conditions as well as the price and toxicity of their constituents, three new HESs thymol + TOPO, TOPO + capric acid and hydrocinnamic acid + capric acid were identified and their full phase diagram and physical properties were characterised. The extraction and selectivity of each system were assessed as a function of metal type, HCl concentration and HES composition. Finally, Pd^{2+} was recovered from the thymol + TOPO HES either *via* a conventional stripping process or by using the HES phase as the template for the synthesis of palladium nanoparticles, highlighting the versatility of non-ionic HESs.

Results and discussion

Physical chemical properties of the Th + TOPO, TOPO + CA and HA + CA systems

From an initial screening of 132 tested mixture points based on 15 different compounds (Fig. S1 and Table S2†), 3 final HES mixtures from the 14 systems obtained (Table S4†) were selected for further study, namely the thymol + TOPO (Th + TOPO), TOPO + capric acid (TOPO + CA) and hydrocinnamic acid + capric acid (HA + CA) HESs. These systems were chosen based on their advantageous thermodynamic properties, low

Table 1 Relevant properties of the pure components used in the studied HES

Compound	T_m (K)	ΔH_m (kJ mol^{-1})	Aqueous solubility (g L^{-1})	LD50 (oral, rat) (mg kg^{-1})[39]	Price ($ kg^{-1})[40]
Thymol	323.5[25]	19.65[25]	0.9[37]	980	10–30
TOPO	325.87[a]	58.02[a]	0.00015[38]	>2000	10–60
Capric acid	304.75[25]	27.5[25]	0.0618[37]	>10 000	8–15
Hydrocinnamic acid	321.75[36]	16.3[36]	5.9[37]	NA	5–30

[a] Determined in this work.

to negligible water solubilities, low toxicity and affordable cost of the pure component, summarized in Table 1, as well as the well-known metal extraction capabilities of carboxylic acids and TOPO for a range of metal ions.[34,35] Furthermore, the choice of these three systems allows for the evaluation of the respective importance of each metal complexing constituent as the Th + TOPO HES solely contains TOPO as the extractant, the HA + CA HES only carboxylic acids and the TOPO + CA HES a mixture of both. Note that although the Th + TOPO system is structurally similar to the previously reported phenol + TOPO system it presents a much lower toxicity and aqueous solubility, the latter for pure phenol in water (82 g L^{-1}) being almost 100 times greater than that of thymol.[27]

The phase diagrams for the Th + TOPO, TOPO + CA and HA + CA mixtures are presented in Fig. 1 and listed in Tables S6 and S7,† along with the ideal solubility curves calculated using eqn (S1).† The activity coefficients derived from eqn (S1) are presented in Fig. S2.† All three hydrophobic mixtures exhibit a phase behaviour characterized by a single eutectic point and possess an extended liquidus compositional range capable of incorporating a significant molar fraction of the TOPO extractant in the cases of the Th + TOPO and TOPO + CA HESs ($0.2 < x_{TOPO} < 0.5$). The SLE phase diagram of the HA + CA mixture presents a quasi-ideal behaviour as previously reported for other carboxylic acid mixtures. The interactions in this HES are comparable to that of its pure components, in line with the tendency of carboxylic acids to form dimers.[41] In contrast, the Th + TOPO and TOPO + CA systems present significant deviations from ideality on both sides of the phase diagram. The TOPO + CA phase diagram is similar to the reported diagram of TOPO + dodecanoic acid.[42] The deviations from thermodynamic ideality presented by both HESs are experimentally represented by the difference of the activity coefficients from unity. The activity coefficients presented in Fig. S2† indicate a greater deviation from 1 on the thymol side of the phase diagram for the Th + TOPO system compared to capric acid in the TOPO + CA system. The large deviations from ideality for non-ionic HESs were previously rationalised based on the significant difference in Lewis acidity between the HBD and HBA resulting in favourable hydrogen-bonding interactions.[9] Phenolic compounds including thymol were identified as inducers of HESs due to the greater acidity of the hydroxyl proton conferred by resonance effects across the aromatic ring. Comparison of the Th + TOPO and phenol + TOPO phase[27] diagrams presented in Fig. S3† shows an almost complete overlap of both, appearing to confirm the ability of phenolic compounds to form HESs. Conversely to the acidity of the phenolic hydroxyl moiety, the phosphine oxide bond of TOPO is highly Lewis basic, even capable of forming liquid coordination complexes with Lewis acidic metal chlorides[43] and

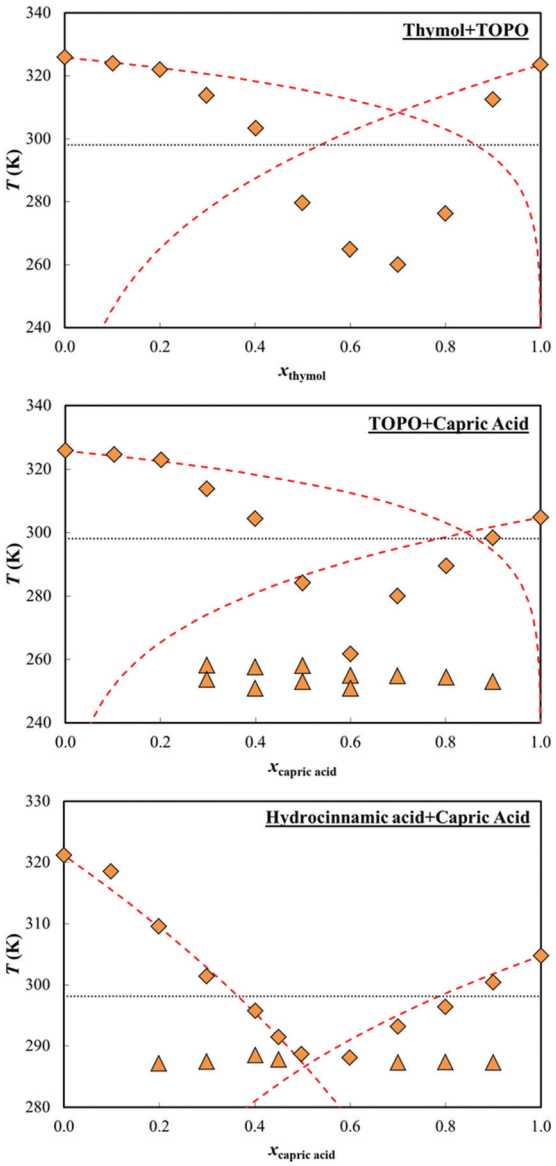

Fig. 1 Phase diagram for the studied mixtures: ♦ melting temperatures, ▲ eutectic temperatures, – – – ideal solubility lines, and ·····T = 298.15 K.

HESs with carboxylic acids (Fig. 1), sulfoxides, diols and thiourea-based compounds.[42] The ability of both thymol and TOPO as HES inducers is further highlighted by the possible number of HES mixtures obtained with either component during the screening phase (Table S4†) and from other studies.[42]

The obtained Th + TOPO, TOPO + CA and HA + CA mixtures at a 1 : 1 molar ratio were investigated and their viscosities and densities were recorded as a function of temperature and are presented in Fig. S4 and S5† respectively and summarised in Table 2. The composition of the eutectic mixtures was confirmed through ^{1}H-NMR spectroscopy, Fig. S6 to S8.† The absence of new peaks in the spectra of the HES relative to the spectra of the pure compounds confirms that no reaction between the mixture components occurred during preparation. Interestingly, the shift corresponding to the hydroxyl moiety of thymol is upshifted by $\Delta\delta$ = 4.1 ppm in the Th + TOPO HES (Fig. S6†), confirming the strong interactions between phenols and phosphine oxides.

The viscosity of all three mixtures, presented in Table 2, is significantly lower than those reported for hydrophobic ionic eutectic mixtures,[21] underlying the advantageous properties of non-ionic HESs. To assess the hydrophobicity and stability of the studied systems, the solubility of water in the eutectic phase was measured directly after preparation and after contact for 24 h with deionized water and 1 M HCl respectively at an O : A volume ratio of 1 (Table 2). The solubility of water in the HES after saturation increases with the concentration of carboxylic acid. When expressed in terms of molar fraction, water represents a non-negligible component of the saturated HES phase, between ~15 and 20 mol%. At such concentrations, water may play an important role in the hydrogen-bonding character and metal solvation of the HES. Equilibration of the Th + TOPO system with increasing HCl concentration was associated with a linear decrease in the water content of the Th + TOPO phase (Fig. S9†). This behaviour is consistent with the reported extraction of mineral acids by basic extractants such as TOPO in an organic solvent, which was found to be solely dependent on the extractant and/or acid concentration and independent of the amount of metal ions extracted.[44–46]

No difference was observed in the ^{1}H-NMR spectra of the HES phase when equilibrated with water or 1 M HCl (Fig. S10 to S15†), confirming its stability under acidic conditions as well as the constant 1 : 1 molar ratio of the components. The spectra of the aqueous phase are in line with the aqueous solubilities of the pure compounds in water listed in Table 1. Hydrocinnamic acid and to a lesser extent thymol are observable in the aqueous phase from their respective HESs whilst no peaks from TOPO or capric acid could be observed. This does not imply that no losses occur but that they are below the ^{1}H-NMR experimental detection limit of approximately 5 mol%. Although the exact solubility of HESs in water was not determined, previous works on non-ionic HESs reported a decrease of one to two orders of magnitude in the aqueous solubility of the most water-soluble components compared to the solubility of their pure state and can therefore be assumed as negligible in the three mixtures.[25,27]

Table 2 Viscosity and density of the Th + TOPO, TOPO + CA and HA + CA mixtures at 298 K and a 1 : 1 molar ratio. The water content in the HES phase was measured after preparation and after contact for 24 h with deionized water (W-HES) and a 1 M HCl solution (A-HES)

HES	Viscosity (mPa s)	Density (g cm^{-3})	Water content (mol.%) HES/W-HES/A-HES
Th + TOPO	69.93	0.898	2.33/15.1/13.8
TOPO + CA	44.11	0.881	1.98/19.2/19.8
HA + CA	11.29	0.978	2.62/20.3/16.0

Metal extraction in carboxylate-based HESs

The Th + TOPO, TOPO + CA and HA + CA mixtures were evaluated for their potential to separate the PGMs Pt^{4+} and Pd^{2+} from selected transition metals commonly found in waste printed circuit boards and three-way catalyst leachates, namely Fe^{3+}, Cr^{3+}, Cu^{2+}, Co^{2+} and Ni^{2+}.[32] Phase disengagement in the HA + CA system proved difficult even after centrifugation, an issue not encountered in the TOPO-based HES. This is most probably due to the closer density of HA + CA with water compared to the other two HESs. The distribution factor of Pt^{4+}, Pd^{2+}, Fe^{3+} and Cu^{2+} as a function of HES selection and HCl concentration is presented in Fig. 2, with all distribution factors listed in Table S8.† To aid the discussion, the metallic species present in aqueous solution at three different chloride concentrations (0.05 M, 1 M and 2 M) are listed in Table S9.† Metal ion (M^{n+}) distribution coefficients (D_M) and the separation factor between two given metals ($\alpha_{M1/M2}$) are calculated using eqn (1) and (2).

$$D_M = \frac{[M]_{HES,f}}{[M]_{aq,f}} = \frac{([M]_{aq,in} - [M]_{aq,f})}{[M]_{aq,f}} \times \frac{V_{aq}}{V_{HES}} \quad (1)$$

$$\alpha_{M1/M2} = \frac{D_{M1}}{D_{M2}} \quad (2)$$

where the subscript HES and aq denote the phase and in and f the time frame (in – before extraction and f – after extraction). Ni^{2+} and Cr^{3+} were not significantly extracted under any of the tested conditions whilst Co^{2+} was only partially extracted at 2 M HCl in the TOPO + CA system (D_{Co} = 0.22 ± 0.04).

Focusing first on the entirely carboxylate-based HA + CA mixture, the system presents the greatest affinity for Fe^{3+} in the absence of HCl (D_{Fe} = 26.7 ± 1.1). Although comparatively lower, the HA + CA also presents the highest extraction of Cu^{2+} of all three HESs under the tested conditions (D_{Cu} = 0.30 ± 0.02 in H_2O). An increase in the acidity of the aqueous solution engenders a corresponding decrease in the extraction of all studied metals for the HA + CA HES, with no significant metal extraction recorded when [HCl] ≥ 1 M. The order of metal extraction for carboxylic acids in organic solvents typically decreases through the series $Pd^{2+} > Fe^{3+} > Cr^{3+} > Cu^{2+} > Ni^{2+} > Co^{2+}$, in accordance with the trend in the first complexation constant of the respective metal with carboxylate anions such

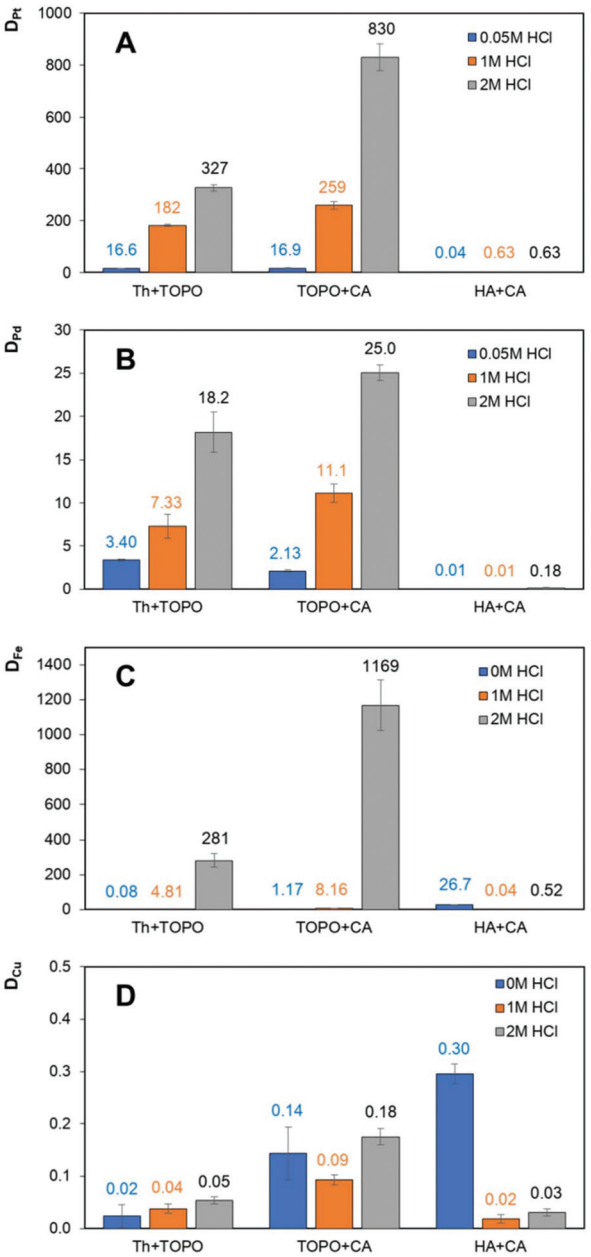

Fig. 2 Distribution coefficient of Pt^{4+}, Pd^{2+}, Fe^{3+} and Cu^{2+} as a function of HES selection and HCl concentration ([Pt^{4+}] = [Pd^{2+}] = 2 mM; [Fe^{3+}] = [Cu^{2+}] = 10 mM; O : A = 0.5; 1 : 1 HES molar composition).

as acetate.[34] The TOPO + CA and HA + CA HESs present similar extraction tendencies: $Fe^{3+} \gg Cu^{2+} \gg Cr^{3+} > Co^{2+} \approx Ni^{2+}$ (pH ≈ 4.9 for divalent metals and pH ≈ 3.0 for trivalent metals). The presence of Cr^{3+} resulted in the emulsification of the HA + CA phase and could not be accurately determined. The absence of PGM extraction in the HA + CA system is assigned to the unfavourable electrostatic interactions between the anionic platinate and palladate chloro-complexes (Table S9†) and the carboxylate ligands.

Carboxylic acid extractants present a pH dependent extraction behaviour typically assigned to the formation of metal–carboxylate complexes and the release of acidic protons to the aqueous phase.[34] The UV-vis spectrum of the turquoise TOPO + CA phase following the extraction of Cu^{2+} at pH = 4.9 presents a peak at 680 nm (Fig. S16†), indicative of a partially dehydrated copper carboxylate complex. UV-vis spectra were not recorded in the other HESs due to spectral overlap from the aromatic groups. It is likely that multiple extraction mechanisms can simultaneously occur in these complex extraction systems. The possibility of anion-exchange during metal extraction at pH 4.9, which is approximately equal to the pK_a of the studied carboxylic acids, cannot be excluded and might explain some of the observed pH-dependence of the extraction behavior. Furthermore, the observed UV-vis spectrum corresponds only to the complexes with the highest extinction coefficients and can mask other species present. Overall, HA + CA exhibits high selectivity for Fe^{3+} in H_2O, with a separation factor with Cu^{2+} of $\alpha_{Fe/Cu}$ = 90.4 and $\alpha_{Fe/M}$ > 200 for the other metals tested. However, the increased loss of the carboxylic acid component under neutral or alkaline conditions could restrict the applicable range of these HESs. The solubility of sodium carboxylate salts is significantly greater than that of their protonated acid.[47]

Metal extraction in phosphine oxide-based HESs

A markedly different trend is observed in the TOPO-based systems. They present good to excellent extraction of the PGMs Pt^{4+} and Pd^{2+} in the tested HCl concentration range and for Fe^{3+} when [HCl] ≥ 2 M (Fig. 2). The distribution of Pt^{4+}, Pd^{2+}, Fe^{3+}, Cu^{2+} and Co^{2+} is dependent on the HCl concentration. For example, in the Th + TOPO system it increases from D_{Pt} = 16.6, D_{Pd} = 3.40 and D_{Fe} = 0.08 in aqueous solution to D_{Pt} = 327, D_{Pd} = 18.2 and D_{Fe} = 281 at 2 M HCl. Whilst no notable extraction of the other metal ions beyond Pt^{4+}, Pd^{2+} and Fe^{3+} was recorded in the Th + TOPO system, the TOPO + CA system presented an increase in Cu^{2+} (D_{Cu} = 0.18 ± 0.02) and Co^{2+} (D_{Co} = 0.22 ± 0.04) partitioning when [HCl] ≥ 2 M characterised by the appearance of golden and blue colours in the DES phase, respectively. The metal extraction affinity of the TOPO-based eutectics follows that of pure TOPO diluted in organic solvents. Although no study directly comparing all the metals assessed in this work was found, metal extraction using TOPO or Cyanex 923 (a mixture of different phosphine oxides) follows the general trend $Pt^{4+} > Pd^{2+} > Fe^{3+} > Zn^{2+} > Fe^{2+} > Co^{2+} \approx Cu^{2+} \gg Ni^{2+} \approx Cr^{3+}$.[48–52] The dominant role of TOPO in the extraction is further validated by comparing the distribution ratio in the TOPO-based eutectics at 2 M HCl in Fig. 2 to those obtained in the HA + CA system for which no significant metal extraction was recorded.

Contrary to carboxylic acid ligands, TOPO is a solvating type extractant, with the extraction in organic diluents depending on the metal complexes present in the aqueous phase (Table S9†). Typically, only the more lipophilic complexes of lower charge densities partition to the organic phase accompanied by the co-extraction of ions with appropriate counter-charge to maintain electroneutrality.[50,53] Both PGM ions are efficiently extracted due to their presence as either

neutral or anionic chlorometalate complexes for all tested HCl concentrations. The increased extraction of Fe^{3+} and Cu^{2+} in the TOPO + CA eutectic at 2 M HCl corresponds to the emergence of their respective neutral complex in aqueous solution (Table S9†). However, the neutral complexes represent but a small percentage of the species distribution and cannot solely explain the large increase in the Fe^{3+} partition.[45,54] The UV-vis spectra of the TOPO + CA phase after extraction of 10 mM Pd^{2+} or Cu^{2+} from a 2 M HCl solution present bands previously assigned to their anionic and neutral complexes (Fig. S16†), suggesting the co-existence of multiple extraction mechanisms. Furthermore, the relatively important molar concentration of water in the HES phase (Table 2) allows for a number of solvated metal complex and counter-ion configurations, namely solvent separated ion-pairs, contact ion-pairs or aggregate structures. Although the species distribution in the eutectic phase cannot be accurately determined, the results suggest that an essential criterion for extraction in TOPO-based eutectics is the partial dehydration of the metal ion first coordination sphere, manifested by a change in the geometry of the complex. This in turn increases the strength of the Lewis acid–base adduct formation in the eutectic phase and favours extraction.[45,53]

Based on the distribution results in Fig. 2 and Table S8,† the selectivity for Pd^{2+} ($\alpha_{Pd/M}$) in the Th + TOPO and TOPO + CA eutectic systems was calculated and is presented in Table 3. Due to the negligible Pd^{2+} extraction in the HA + CA eutectic, the separation factor in this system was not evaluated. Below 1 M HCl, the Th + TOPO system presents the greatest selectivity for PGMs over transition metals including Fe^{3+} ($\alpha_{Pd/Fe}$ = 41) and Cu^{2+} ($\alpha_{Pd/Cu}$ = 140), allowing for the selective recovery of PGMs from complex matrices. Furthermore, the greater distribution factor for Pt^{4+} over Pd^{2+} in TOPO-based eutectics suggests the possibility of inter PGM separation. Such a possibility will be explored in a future work. PGM distribution and selectivity in the presented TOPO-based mixtures compare favourably with those reported for TOPO in diluents or ILs whilst avoiding the use of fluorinated moieties and/or organic solvents.[44,50,52,55–57]

It appears that HESs retain some of the metal complexing characteristics of their individual components in organic diluents. This allows for the predictable preparation of mixtures capable of extracting metals under a range of conditions by two different mechanisms, such as for the extraction of Fe^{3+} and Cu^{2+} in the TOPO + CA eutectic. Under less acidic conditions, extraction proceeds *via* the formation of carboxylate–metal complexes whilst at higher HCl concentrations TOPO dictates the extraction. Such behaviour contradicts the often held belief that in binary eutectic solvents one component is responsible for the decrease of the melting point whilst the other is the "active" component, thereby opening the possibility for synergistic hydrophobic eutectics. For a given metal ion, extraction can be further tailored by addition of various counter-ions like perchlorates (ClO_4^-) or acetate (CH_3COO^-) that can promote certain extraction pathways as exemplified for Cu^{2+} extraction in Fig. 3.

Influence of HCl concentration and HES composition on palladium extraction

To gain further insight into the extraction of PGMs in TOPO-based HESs, the extraction of Pd^{2+} in the Th + TOPO eutectic as a function of HCl concentration was assessed and the extraction was followed by ^{31}P-NMR of the Th + TOPO phase, Fig. 4. The Th + TOPO eutectic was selected to simplify the extraction mechanism interpretation compared to the TOPO + CA systems composed of two possible metal ligands. The distribution curve of Pd^{2+} with HCl concentration in the Th + TOPO system, Fig. 4A, presents a concave shape with a minimum at 0.5 M HCl and increases thereafter with increasing HCl concentration. A similar behaviour was reported for

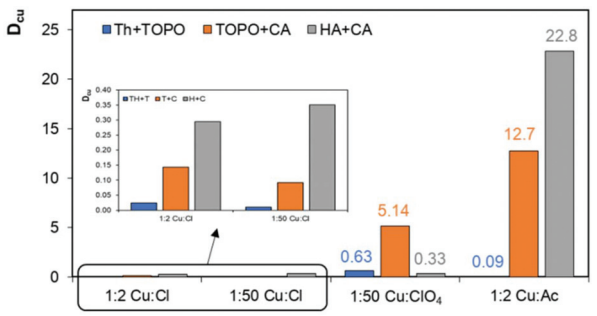

Fig. 3 Distribution coefficient of Cu^{2+} as a function of HES selection and sodium salt addition ([Cu^{2+}] = 10 mM; O : A = 0.5; 1 : 1 HES molar composition, pH = 4.9).

Table 3 Separation factor of Pd^{2+} from other metals ($\alpha_{Pd/M}$) in the Th + TOPO and TOPO + CA systems as a function of HCl concentration (for metals with D_M < 0.02, a $\alpha_{Pd/M}$ > 200 was applied)

	0 M HCl		1 M HCl		2 M HCl	
$\alpha_{Pd/M}$	Th + TOPO	TOPO + CA	Th + TOPO	TOPO + CA	Th + TOPO	TOPO + CA
Pd/Pt	0.20	0.13	0.04	0.04	0.06	0.03
Pd/Cu	140	14.8	191	119	337	143
Pd/Co	>200	74.75	>200	525	>200	113
Pd/Ni	>200	>200	>200	>200	>200	>200
Pd/Cr	38.2	13.3	>200	>200	>200	>200
Pd/Fe	41.0	1.81	1.52	1.36	0.06	0.02

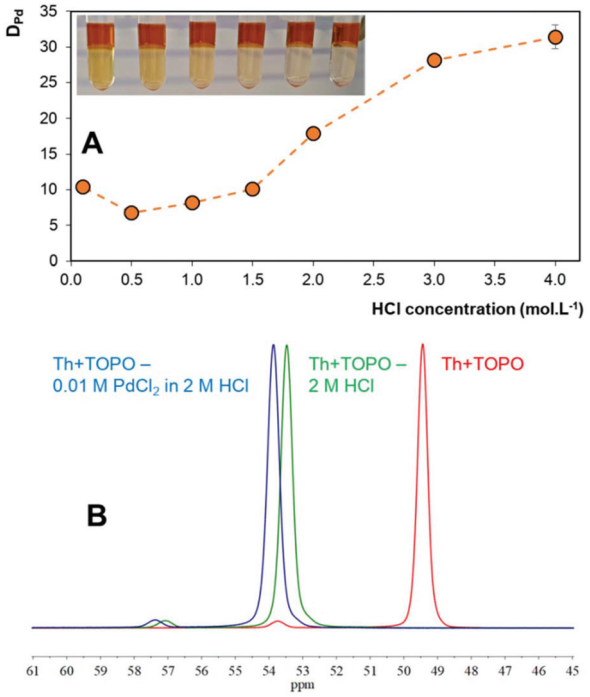

Fig. 4 (A) Distribution of Pd^{2+} in the Th + TOPO eutectic as a function of HCl concentration. The inset picture shows the HES after extraction with increasing HCl concentration from left (0.5 M HCl) to right (4 M HCl). (B) ^{31}P-NMR of the Th + TOPO eutectic phase after preparation (red), after coming into contact with 2 M HCl (green) and after extraction of Pd^{2+} from a 2 M HCl solution (blue). Extraction conditions: [Pd^{2+}] = 10 mM, O : A = 0.5 and x_{TOPO} = 0.5.

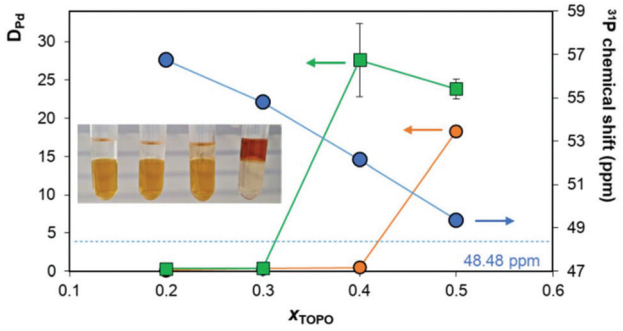

Fig. 5 Distribution of Pd^{2+} in the Th + TOPO system (circles) and TOPO + CA system (squares) and the ^{31}P-NMR chemical shift of TOPO in the pure Th + TOPO eutectic as a function of the TOPO molar fractions (x_{TOPO}). The dashed line represents the ^{31}P-NMR shift of TOPO in $CDCl_3$. The inset picture shows the Th + TOPO HES after extraction at the four x_{TOPO} tested increasing from left to right. Extraction conditions: [Pd^{2+}] = 10 mM, O : A = 0.5 and [HCl] = 2 M HCl.

Pd^{2+} extraction using 0.10 M TOPO in *o*-xylene and is consistent with the change in palladium coordination (Table S9†), and therefore the extraction mechanism, with chloride concentration.[44,50]

Fig. 4B presents the ^{31}P-NMR analysis of the Th + TOPO eutectic phase before and after equilibrating with 2 M HCl solution and after extraction of 10 mM $PdCl_2$. A large positive shift in the peak associated with the phosphine oxide moiety after coming into contact with HCl is observed, showing the important interaction between TOPO and H^+. The surface enrichment of the amphiphilic TOPO at the organic–aqueous interface and its interaction with ions, including H^+ and counter-anions, were shown to be a determining factor of the interfacial transport of metal ions, ultimately influencing their extraction.[58,59] The change in the HES–aqueous interface with increasing HCl could facilitate the partition of metal complexes to the HES phase. Addition of $PdCl_2$ engenders an additional positive shift in the ^{31}P-NMR of TOPO despite the large molar excess of TOPO to Pd^{2+} in the system (approximately 86 : 1), suggesting a direct interaction of TOPO with the metal ion centre.

An important advantage of eutectic solvents is the capacity to adjust both the mixture components and their respective molar ratio. To better appreciate this, the extraction of Pd^{2+} as a function of the eutectic molar composition was studied in both TOPO systems, Th + TOPO and TOPO + CA. The distribution results are presented in Fig. 5 alongside the ^{31}P-NMR chemical shift of TOPO in the pure Th + TOPO eutectic for various TOPO molar fractions (x_{TOPO}). Only molar compositions in the room-temperature liquidus range were studied. The distribution of Pd^{2+} in both Th + TOPO and TOPO + CA HES presents a compositional threshold below which no extraction occurs. The x_{TOPO} threshold for extraction as well as the distribution value depends on the selection of the second eutectic component. The TOPO + CA HES presents both higher D_{Pd} values and a larger extraction range ($x_{TOPO} > 0.3$) compared to the Th + TOPO HES ($x_{TOPO} > 0.4$), in line with the distribution results in Fig. 2. Importantly, D_{Pd} in both HESs under optimised conditions (Fig. 4 and 5) is comparable or superior to reported values for 1 mM Pd^{2+} extraction using 0.1 M TOPO diluted in chloroform, cyclohexane, methyl isobutyl ketone (MIBK), 2,2′-dichlorodiethyl ether[55] or *o*-xylene[44] for a given HCl concentration.

The presented results in Fig. 4 and 5 reinforce the image of non-ideal HESs as complex extraction systems exhibiting a conflicting duality. On one hand, the "on/off" Pd^{2+} extraction behaviour in Fig. 5 is markedly different to that observed using TOPO in organic diluents which increases predictably with TOPO concentration.[44,50,52,55] Additionally, no such behaviour was reported for metal extraction in HESs presenting no significant deviations from thermodynamic ideality.[26] On the other hand, for HES composition at which Pd^{2+} extraction does occur, the distribution profile of D_{Pd} in Th + TOPO with HCl, Fig. 4, is similar to that obtained using TOPO in *o*-xylene.[44,50,55] The relationship between the stability of the eutectic phase and its impact on metal extraction is best exemplified by following the ^{31}P-NMR chemical shift of TOPO in the Th + TOPO eutectic as a function of x_{TOPO} (Fig. 5). A decrease in x_{TOPO} yields an upshift in the ^{31}P-NMR chemical shift of TOPO. This is indicative of the P═O bond in a more deshielded environment and consistent with the increasing concentration of the acidic H-bond thymol. Only when an

"excess" of TOPO is present such that its ^{31}P-NMR shift in the Th + TOPO HES approaches that of pure TOPO in $CDCl_3$ does extraction occur.

Relating the HES structure to extraction

The relation between HES non-ideality and metal extraction is addressed further in this section, focusing on the relative importance of the second component in TOPO-based HESs. The differences in the distribution coefficient and operational composition range are attributed to variations in intermolecular interactions between the HES components. As TOPO is common to Th + TOPO and TOPO + CA eutectics, the comparison of both systems can be simplified for the study of the second component with itself and with TOPO respectively. Molecular dynamics (MD) analysis for x_{TOPO} = 0.5 of the Th + TOPO system (Fig. 6A) confirms the dominant nature of the TOPO–thymol H-bond interaction compared to thymol–thymol aggregation – for both short and longer range ordering as evidenced by the larger coordination numbers (CN). In contrast, Fig. 6C indicates an important inter-carboxylic interaction in the TOPO + CA HES at the expense of TOPO-capric acid H-bonding, with the former being more prominent short range interaction ($r \leq 0.4$ nm). MD results are supplemented by gas-phase density functional theory (DFT) calculations of the eutectic pair between tributylphosphine oxide (TBPO) with thymol and pentanoic acid (PA) respectively. The final optimised geometries are shown in Fig. 6B and D. Although the alkyl chain lengths were reduced to decrease the computational time, conclusions drawn from the DFT results are transferable to the TOPO systems as the functional groups of interest are identical. Interestingly, the TBPO–thymol and TBPO–pentanoic acid eutectic pairs present similar counterpoise corrected energy values of ΔE(TBPO + Th) = −83.2 kJ mol^{-1} and ΔE(TBPO + PA) = −82.8 kJ mol^{-1}. Both eutectic pairs are characterised by delocalisation of the hydrogen-bond critical point away from TBPO towards the second component (Fig. 6). However, the inter-phenolic H-bonding (ΔE(Th + Th) = −46.6 kJ mol^{-1}) is weaker respective to the inter-carboxylate one (ΔE(PA + PA) = −79.0 kJ mol^{-1}). MD simulations of the Th + TOPO system for x_{TOPO} varying from 0.2 to 0.5 indicate a non-linear increase in the thymol(OH)–TOPO(P═O) CN with decreasing x_{TOPO} (Fig. 7A). The relative increase in the (P═O)-(OH) CN for short range interactions typically corresponding to H-bonding ($r \leq 0.3$ nm) reaches a plateau for x_{TOPO} < 0.4. This threshold corresponds to a thymol : TOPO ratio of approximately 2, with a further increase in the CN limited by steric effects. In contrast the thymol(OH)–thymol(OH) CN increases linearly (Fig. 7B) with decreasing x_{TOPO}.

Non-ionic HESs are characterised by H-bonding, with the strength of the H-bond between the HBD and HBA relative to in the pure compounds influencing the non-ideality of the system. For extraction to occur, the strength of the ligand–metal complex must be equal to or greater than other possible interactions, including overcoming the H-bonding interactions between the HES components. Simulation results indicate that Th + TOPO and TOPO + CA should present similar interaction energies between the HBD and HBA (Fig. 6). However, the competing interaction of the carboxylic dimer at the expense of TOPO–CA interaction liberates TOPO to interact with the metal complex. This confers TOPO + CA larger D_{Pd} values and a greater compositional extraction range compared to Th + TOPO, in which TOPO is restricted by the phosphine oxide-phenol H-bond. This subtle difference is identified as the

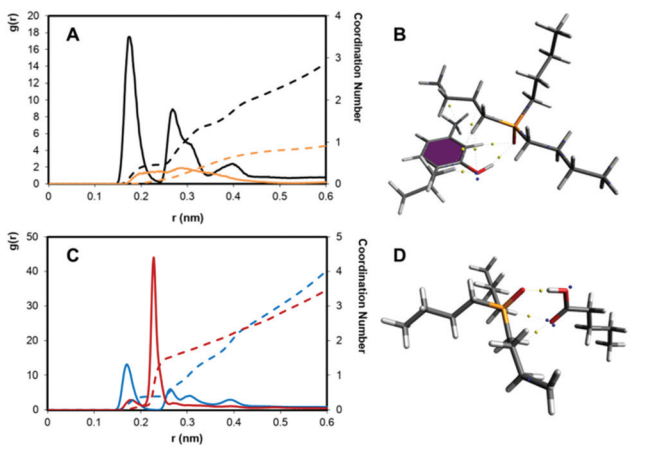

Fig. 6 Left panels: RDFs (solid lines) and coordination numbers (dashed lines) between the polar groups (P═O for TOPO, OH for thymol and OOH for capric acid) of (A) TOPO–Th (black) and Th–Th (orange) in the 1 : 1 Th + TOPO HES and of (C) TOPO–CA (blue) and CA–CA (red) in the 1 : 1 TOPO + CA HES. Right panels: QTAIM representation of the gas-phase DFT optimized (B) TBPO–Th and (D) TBPO–PA pairs at the M062X/6-311++G(d,p) level of theory (small yellow/blue dots indicate bond critical points/lone pairs).

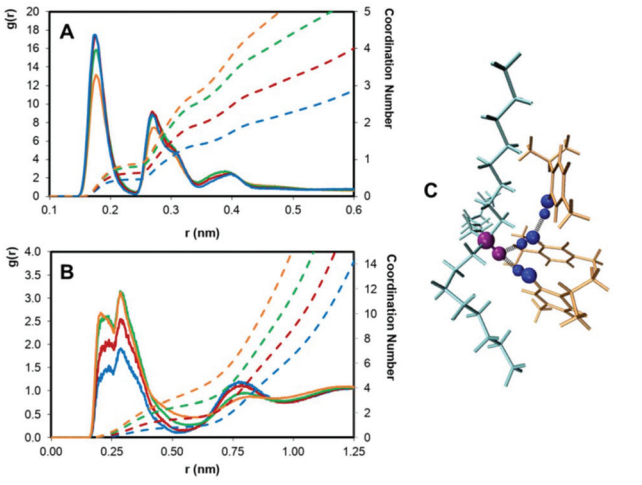

Fig. 7 RDFs (solid lines) and coordination numbers (dashed lines) between (A) TOPO (P═O group) with thymol (OH group) and (B) thymol with thymol (OH groups) in the 1 : 1 Th + TOPO HES at various x_{TOPO} molar fractions (x_{TOPO} = 0.5 – blue, x_{TOPO} = 0.4 – red, x_{TOPO} = 0.3 – green, and x_{TOPO} = 0.2 – orange). (C) Representative example of TOPO–thymol coordination in the Th + TOPO HES at x_{TOPO} = 0.2 (TOPO – cyan, P═O group of TOPO – purple, thymol – orange, and OH group of thymol – blue).

primary cause for the D_{Pd} differences observed in the Th + TOPO and TOPO + CA systems. Furthermore, the decrease of x_{TOPO} in the Th + TOPO system results in the incorporation of TOPO in a larger hydrogen bonded network with bridging thymol molecules (Fig. 7C). This "trapping" of TOPO by thymol increases the energetic barrier for TOPO–metal ion interaction and restricts the compositional extraction range as shown in Fig. 5. Relating these insights to metal extraction, it appears that a compromise must be made between the loading capacity and compositional extraction range of HESs against their selectivity for a given metal. "Deep" HESs, *i.e.* those presenting strong HBA–HBD hydrogen bonding, can restrict the total extraction capacity as the energy of the metal-extraction complex must overcome the stability of the eutectic pair. However, this greater energy barrier can be used advantageously to increase the HES selectivity at the expense of a lower loading capacity as shown in Table 3 for the Th + TOPO system compared to the TOPO + CA HES. The latter exhibits higher distribution coefficients but lower selectivity values for Pd^{2+}. Fig. 5 stresses the importance of relating the HES extraction to the phase diagram: studies focusing on an arbitrarily selected eutectic mixture composition can miss important trends.

Metal stripping, HES recovery and valorisation of extracted products

Having demonstrated the extraction mechanism of Pd^{2+} in TOPO-based HESs, two methodologies for its recovery from the Th + TOPO phase following extraction from a 1 M HCl solution are here presented. The first methodology is a conventional stripping step whilst the second makes use of the HES phase as a sacrificial template for Pd nanoparticle synthesis based on the ability of TOPO to act as a capping agent.[60] This exploratory study is meant to emphasise the versatility of HESs, with a more systematic assessment of these approaches envisaged in future works. Following extraction of 10 mM $PdCl_2$ from a 1 M HCl solution, the loaded Th + TOPO phase was easily stripped with 96% efficiency using an acidic 0.1 M thiourea solution (O : A = 0.25, [HCl] = 0.5 M). ^{1}H-NMR of the regenerated HES phase in Fig. S17† confirms (i) the absence of thiourea despite the reported formation of TOPO + *N*,*N*′-dihexylthiourea HES[42] and (ii) the constant 1 : 1 TOPO–thymol molar ratio, validating the minimal loss of either HES constituent during extraction.

Alternatively, the Th + TOPO phase after extraction was isolated, vigorously mixed for 5 min with a 0.1 M $NaCH_3COO$ aqueous solution (O : A = 0.5) and left to stand at room temperature. A progressive darkening of the aqueous phase was observed with time. The UV-vis spectra of the aqueous phase (Fig. S18†) present the absence of peaks above 300 nm compared to $PdCl_2$ in 1 M HCl but one peak at 278 nm, suggesting the incomplete reduction of all palladium ions in solution. After three days of standing, the aqueous phase was collected and analysed by TEM (Fig. 8), and the formation of evenly sized but irregularly shaped palladium nanoparticles with an average size of 5.7 ± 1.3 nm was observed based on 80 independent measurements. Contacting the loaded HES phase with an aqueous $NaCH_3COO$ solution yields a substitution of the chloride ligands of the palladium complexes coordinated by TOPO in the HES phase $[Pd(Cl)_x(TOPO)_y]$ by acetate anions, resulting in the formation of intermediate complexes expressed as $[Pd(CH_3COO)_x(TOPO)_y]$. The slow diffusion of the acetate anion in the HES combined with the large molar excess of TOPO to palladium ensures a kinetic-controlled growth of palladium nanoparticles obtained under ambient conditions and in the absence of additional solvents. A similar nanoparticle growth regime was observed for other Lewis basic capping agents such as oleylamine in which the kinetics of growth were slowed by altering the nature of the intermediate complex through increasing oleylamine concentration.[61] Interestingly, these results could not be reproduced in the TOPO + CA HES under the same experimental conditions. Although both recovery approaches proposed here are just proof-of-concepts that require further investigation and optimization, they serve to illustrate the potential of HESs not only as recyclable media for metal extraction but also for the direct production of value added components by careful selection of the HES component.

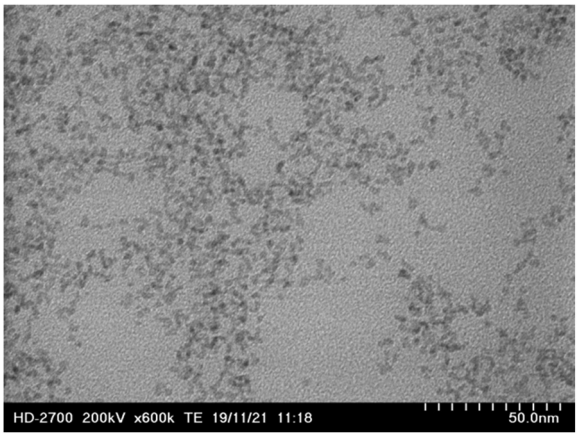

Fig. 8 TEM analysis of the palladium nanoparticles obtained from the loaded Th + TOPO phase after coming into contact with a 0.1 M $NaCH_3COO$ aqueous solution (contact time = 72 h, O : A = 0.5, x_{TOPO} = 0.5).

Conclusions

This work expands the potential of non-ionic HESs, positioning them as integrated extraction-separation platforms for the purification of various metal ions through judicious selection of the HES components. Starting from a large screening of possible mixtures, three eutectic solvents based on either phosphine oxide or carboxylate ligands and bio-sourced compounds were identified and characterised. These HESs present low viscosities and high hydrophobicity suitable for solvent extraction processes, capable of simultaneously acting as the hydrophobic phase and extractant. TOPO-based HESs present

good selectivity towards PGMs over other transition metals in aqueous solution, a selectivity that could be tuned by selection of the second HES component. PGM extraction and selectivity in these HESs compare favourably with those reported for TOPO in diluents or ILs whilst avoiding the use of fluorinated moieties and/or organic solvents. Palladium extraction in TOPO-based HESs depends on a variety of factors – including HCl concentration as well as HES selection and composition. By determining the factors governing extraction, the results presented can be extrapolated to other HES/metal systems, thereby widening the applicability of HESs in solvent extraction. However, more work is required to better understand the possible extraction mechanisms in these complex solvents. Finally, the versatility of HESs is further demonstrated as these can be stripped according to traditional solvent extraction processes or used as a template for the production of high-value nanoparticles. Overall, non-ionic HESs stand out for their great potential as a more environmentally benign alternative to hydrophobic ILs or extracting ligands diluted in organic solvents.

Experimental

A detailed description of the experimental procedure followed in this work is available in the ESI,† including chemicals and instrumentation, screening of hydrophobic eutectic mixtures, characterisation of the selected HESs, thermodynamic modelling of the solid–liquid equilibria, metal extraction in selected HESs, palladium recovery from the Th + TOPO phase and computational protocols.

Conflicts of interest

There are no conflicts to declare.

Acknowledgements

This work was developed within the scope of the project CICECO-Aveiro Institute of Materials, UIDB/50011/2020 and UIDP/50011/2020, financed by national funds through the FCT/MEC and when appropriate co-financed by FEDER under the PT2020 Partnership Agreement. The NMR spectrometers are part of the National NMR Network (PTNMR) and are partially supported by Infrastructure Project No. 022161 (co-financed by FEDER through COMPETE 2020, POCI and PORL and FCT through PIDDAC).

References

1 A. P. Abbott, G. Capper, D. L. Davies, R. K. Rasheed and V. Tambyrajah, *Chem. Commun.*, 2003, 70–71.
2 M. C. Gutierrez, D. Carriazo, C. O. Ania, J. B. Parra, M. Luisa Ferrer and F. del Monte, *Energy Environ. Sci.*, 2011, **4**, 3535–3544.
3 O. S. Hammond, K. J. Edler, D. T. Bowron and L. Torrente-Murciano, *Nat. Commun.*, 2017, **8**, 14150.
4 D. A. Alonso, A. Baeza, R. Chinchilla, G. Guillena, I. M. Pastor and D. J. Ramón, *Eur. J. Org. Chem.*, 2016, 612–632.
5 C. Batarseh, A. Levi-Zada and R. Abu-Reziq, *J. Mater. Chem. A*, 2019, **7**, 2242–2252.
6 E. L. Smith, A. P. Abbott and K. S. Ryder, *Chem. Rev.*, 2014, **114**, 11060–11082.
7 G. García, S. Aparicio, R. Ullah and M. Atilhan, *Energy Fuels*, 2015, **294**, 2616–2644.
8 M. Zdanowicz, K. Wilpiszewska and T. Spychaj, *Carbohydr. Polym.*, 2018, **200**, 361–380.
9 D. O. Abranches, M. A. R. Martins, L. P. Silva, N. Schaeffer, S. P. Pinho and J. A. P. Coutinho, *Chem. Commun.*, 2019, **55**, 10253–10256.
10 A. Söldner, J. Zacha and B. König, *Green Chem.*, 2019, **21**, 321–328.
11 P. Zürner and G. Frisch, *ACS Sustainable Chem. Eng.*, 2019, **75**, 5300–5308.
12 A. P. Abbott, R. C. Harris, F. Holyoak, G. Frisch, J. Hartley and G. R. T. Jenkin, *Green Chem.*, 2015, **17**, 2172–2179.
13 J. M. Hartley, C. M. Ip, G. C. H. Forrest, K. Singh, S. J. Gurman, K. S. Ryder, A. P. Abbott and G. Frisch, *Inorg. Chem.*, 2014, **5312**, 6280–6288.
14 D. J. G. P. van Osch, L. F. Zubeir, A. van den Bruinhorst, M. A. A. Rocha and M. C. Kroon, *Green Chem.*, 2015, **17**, 4518–4521.
15 M. B. Arain, E. Yilmaz, M. Soylak and M. , *J. Mol. Liq.*, 2016, **224**, 538–543.
16 T. E. Phelps, N. Bhawawet, S. S. Jurisson and G. A. Baker, *ACS Sustainable Chem. Eng.*, 2018, **611**, 13656–13661.
17 Y. Shi, D. Xiong, Y. Zhao, T. Li, K. Zhang and J. Fan, *Chemosphere*, 2020, **241**, 125082.
18 Z. Erbas, M. Soylak, E. Yilmaz and M. Dogan, *Microchem. J.*, 2019, **145**, 745–750.
19 S. Ruggeri, F. Poletti, C. Zanardi, L. Pigani, B. Zanfrognini, E. Corsi, N. Dossi, M. Salomäki, H. Kivelä, J. Lukkari and F. Terzi, *Electrochim. Acta*, 2019, **295**, 124–129.
20 E. E. Tereshatov, M. Y. Boltoeva and C. M. Folden III, *Green Chem.*, 2016, **18**, 4616–4622.
21 C. Florindo, L. C. Branco and I. M. Marrucho, *ChemSusChem*, 2019, **12**, 1549–1559.
22 L. P. E. Macário, H. Oliveira, A. C. Menezes, S. P. M. Ventura, J. L. Pereira, A. M. M. Gonçalves, J. A. P. Coutinho and F. J. M. Gonçalves, *Sci. Rep.*, 2019, **9**, 3932.
23 D. J. G. P. van Osch, D. Parmentier, C. H. J. T. Dietz, A. van den Bruinhorst, R. Tuinier and M. C. Kroon, *Chem. Commun.*, 2016, **52**, 11987–11990.
24 M. A. R. Martins, L. P. Silva, N. Schaeffer, D. O. Abranches, G. J. Maximo, S. P. Pinho and J. A. P. Coutinho, *ACS Sustainable Chem. Eng.*, 2019, **720**, 17414–17423.

25 M. A. R. Martins, E. A. Crespo, P. V. A. Pontes, L. P. Silva, M. Bülow, G. J. Maximo, E. A. C. Batista, C. Held, S. P. Pinho and J. A. P. Coutinho, *ACS Sustainable Chem. Eng.*, 2018, **6**, 8836–8846.
26 N. Schaeffer, M. A. R. Martins, C. M. S. S. Neves, S. P. Pinho and J. A. P. Coutinho, *Chem. Commun.*, 2018, **54**, 8104–8107.
27 M. Gilmore, E. N. McCourt, F. Connolly, P. Nockemann, M. Swadźba-Kwaśny and J. D. Holbrey, *ACS Sustainable Chem. Eng.*, 2018, **6**, 17323–17332.
28 G. M. Mudd, Sustainability Reporting and the Platinum Group Metals: A Global Mining Industry Leader?, *Platinum Metals Rev.*, 2012, **56**, 2–19.
29 European Commission, *Report on critical material for the EU*, COM(2017)-490, Brussel, 2017.
30 J. Zhang, M. P. Everson, T. J. Wallington, F. R. Field III, R. Roth and R. E. Kirchain, *Environ. Sci. Technol.*, 2016, **50**, 7687–7695.
31 M. Saurat and S. Bringezu, *J. Ind. Ecol.*, 2008, **12**, 754–767.
32 Y. Ding, S. Zhang, B. Liu, H. Zheng, C. C. Chang and C. Ekberg, *Resour., Conserv. Recycl.*, 2019, **141**, 284–298.
33 D. J. G. P. van Osch, C. H. J. T. Dietz, J. van Spronsen, M. C. Kroon, F. Gallucci, M. van Sint Annaland and R. Tuinier, *ACS Sustainable Chem. Eng.*, 2019, **73**, 2933–2942.
34 J. S. Preston, *Hydrometallurgy*, 1985, **14**, 171–188.
35 E. K. Watson and W. A. Rickelton, *Solvent Extr. Ion Exch.*, 1992, **10**, 879–889.
36 M. Iwahashi, S. Takebayashi, A. Umehara, Y. Kasahara, H. Minami, H. Matsuzawa, T. Inoue and H. Takahashi, *Chem. Phys. Lipids*, 2004, **129**, 195–208.
37 R. M. Dannenfelser and S. H. Yalkowsky, *Sci. Total Environ.*, 1991, **109–110**, 625–628.
38 S. M. Elwaer, *Czech. J. Phys.*, 2003, **53**, 497–499.
39 SigmaAldrich Chemical SDS. https://www.sigmaaldrich.com/[Accessed: 28/02/2020].
40 Alibaba, https://www.alibaba.com/[Accessed: 28/02/2020].
41 M. C. Costa, M. Sardo, M. P. Rolemberg, J. A. P. Coutinho, A. J. A. Meirelles, P. Ribeiro-Claro and M. A. Krähenbühl, *Chem. Phys. Lipids*, 2009, **160**, 85–97.
42 A. van den Bruinhorst, S. Raes, S. A. Maesara, M. C. Kroon, A. Catarina, C. Esteves and J. Meuldijk, *Sep. Purif. Technol.*, 2019, **216**, 147–157.
43 J. M. Hogg, L. C. Brown, A. Matuszek, P. Latos, A. Chrobok and M. Swadzba-Kwasny, *Dalton Trans.*, 2017, **46**, 11561–11574.
44 Y. Hasegawa, I. Kobayashi and S. Yoshimoto, *Solvent Extr. Ion Exch.*, 1991, **9**, 759–768.
45 R. Lommelen, T. Vander Hoogerstraete, B. Onghena, I. Billard and K. Binnemans, *Inorg. Chem.*, 2019, **58**, 12289–12301.
46 D. S. Flett, *J. Organomet. Chem.*, 2005, **690**, 2426–2438.
47 A. N. Campbell and G. R. Lakshminarayanan, *Can. J. Chem.*, 1965, **43**, 1729–1737.
48 T. Saito and M. Yamatake, *Z. Anorg. Allg. Chem.*, 1972, **391**, 174–182.
49 J. Saji, T. Prasada Rao, C. S. P. Iyer and M. L. P. Reddy, *Hydrometallurgy*, 1998, **49**, 289–296.
50 Y. Surakitbanharn, S. Muralidharan and H. Freiser, *Solvent Extr. Ion Exch.*, 1991, **9**, 45–59.
51 K. Larsson, C. Ekberg and A. Ødegaard-Jensen, *Hydrometallurgy*, 2012, **129–130**, 35–42.
52 B. Gupta and I. Singh, *Hydrometallurgy*, 2013, **134–135**, 11–18.
53 J. Rydberg, G. R. Choppin, C. Musikas and T. Sekine, Solvent extraction equilibria, in *Solvent Extraction Principles and Practice*, ed. J. Rydberg, Marcel Dekker, New York, 2nd edn, 2004.
54 W. Liu, B. Etschmann, J. Brugger, L. Spiccia, G. Foran and B. McInnes, *Chem. Geol.*, 2006, **231**, 326–349.
55 M. Mojski, *J. Radioanal. Chem.*, 1978, **46**, 239–245.
56 S. Katsuta, Y. Yoshimoto, M. Okai, Y. Takeda and K. Bessho, *Ind. Eng. Chem. Res.*, 2011, **50**(22), 12735–12740.
57 N. Papaiconomou, L. Svecova, C. Bonnaud, L. Cathelin, I. Billard and E. Chainet, *Dalton Trans.*, 2015, **44**, 20131–20138.
58 P. Sun, K. Huang and H. Liu, *Langmuir*, 2018, **34**, 11374–11383.
59 K. Prochaska, M. Walczak and K. Staszak, *J. Colloid Interface Sci.*, 2002, **248**, 143–148.
60 Z. Niu and Y. Li, *Chem. Mater.*, 2014, **26**(1), 72–83.
61 Z. Niu, Q. Peng, M. Gong, H. Rong and Y. Li, *Angew. Chem., Int. Ed.*, 2011, **50**, 6315–6319.